

Photodecomposition of Phenol in a Flow Reactor: Adsorption and Kinetics

A. Sobczyński^{1,*}, J. Gimenez², and S. Cervera-March²

¹ Faculty of Commodity Science, Poznań University of Economics, PL-60967 Poznań, Poland

² Department of Chemical Engineering, Faculty of Chemistry, University of Barcelona, E-08028 Barcelona, Spain

Summary. In this study, a new air lift loop photoreactor was used for both continuous and non-continuous water photodetoxification. Also, the kinetics of phenol photodegradation were measured under flow conditions. Both the kinetics of phenol adsorption on TiO₂/SiO₂ and of the total photomineralization of phenol were measured in order to gain more knowledge on the photocatalytic oxidation of phenol on illuminated titania.

Adsorption of phenol on TiO₂/SiO₂ proceeds even from diluted solutions. However, based on our data, it is impossible to state precisely the influence of the adsorption on the overall rate of phenol photodecomposition. The photoreaction yields stable intermediates which subsequently undergo total mineralization to CO₂ and H₂O. It is postulated that the intermediates consist mainly of polymeric compounds, difficult to determine by conventional analytical methods like GC, HPLC, or UV/Vis spectroscopy.

Keywords: Phenol photodegradation; Kinetics; Flow reactor.

Photolyse von Phenol in einem Durchflußreaktor: Adsorption und Kinetik

Zusammenfassung. Ein neuartiger Photoreaktor wurde auf seine Verwendbarkeit zur kontinuierlichen und nichtkontinuierlichen Wasseraufbereitung getestet. Die Kinetik des photolytischen Abbaus von Phenol wurde unter Durchflußbedingungen untersucht. Zum besseren Verständnis der photokatalysierten Oxidation von Phenol auf belichtetem Titanoxid wurde außerdem die Kinetik sowohl der Adsorption von Phenol an TiO₂/SiO₂ als auch seiner Gesamtphotomineralisierung erforscht.

Adsorption von Phenol an TiO₂/SiO₂ erfolgt bereits aus verdünnten Lösungen. Nach unseren Ergebnissen ist es allerdings unmöglich, den Einfluß der Adsorption auf die Photolyse genau zu bestimmen. Die Photoreaktion ergibt stabile Zwischenprodukte, die sich im weiteren Verlauf zu CO₂ und H₂O umsetzen. Es wird postuliert, daß es sich bei den Zwischenprodukten hauptsächlich um Polymere handelt, die mit konventionellen analytischen Techniken wie GC, HPLC oder UV/Vis-Spektroskopie schwer nachzuweisen sind.

Introduction

Degradation of phenolic compounds is important from a technical point of view: they constitute major water pollutants, and the degree of their presence in the

environment is restricted by laws. The degradation of these compounds is also of scientific interest owing to their resistivity to oxidation – mineralization of phenol and its derivatives needs opening of aromatic rings. Among many methods that can be utilized for the treatment of phenols and other organic wastes, photocatalysis on semiconductors offers several advantages [1]: (i) the oxidant is atmospheric oxygen and the catalyst, mainly TiO_2 , is not hazardous; (ii) oxidation leads most frequently to total mineralization; and (iii) solar energy can be utilized. Although hundreds of papers have been published dealing with the oxidation of organic compounds in the presence of illuminated semiconductors (see *e.g.* Refs. [2–7] and Refs. cited therein), technical application of the method is still restricted. Attempts to scale up the photoreactors used in laboratory experiments have not yet resulted in efficient technical scale systems for water photodetoxification [8–10].

Many papers have been published dealing with the kinetics of photooxidation of various organic wastes in water including phenols [1, 11, 12–26]. From the beginning up to now, the photocatalytic process has been regarded most frequently to be governed by a *Langmuir-Hinshelwood* mechanism. Appropriate kinetic expressions have been derived basing on experimental findings. It has been shown, however, that the reaction can be fitted roughly to the *Langmuir-Hinshelwood* equation independent of the reaction mechanism [27]. In other words, not only the reaction between two adsorbed species obeys the equation, but the same equation can be applied successfully even when desorbed OH radicals react with organic molecules in a bulk solution. Both mechanisms have been proved experimentally. Phenol adsorption on a semiconductor surface has indeed been observed [11, 28, 29]. On the other hand, free OH radicals have been determined by ESR spectroscopy in an irradiated slurry of titania [30]. Moreover, it has been shown by *Goldstein et al.* [31] that the reaction can proceed *via* two different routes. At relatively low phenol concentrations the photoreaction proceeds *via* photochemically induced OH radicals. At higher phenol concentrations a direct reaction takes place between photogenerated holes and adsorbed phenol molecules. The direct reaction route has been also confirmed by other authors [32].

In this paper, the kinetics of the photocatalytic oxidation of phenol on illuminated $\text{TiO}_2/\text{SiO}_2$ particles under flow conditions using a previously described fluidized bed photoreactor are discussed [33]. Also, the adsorption of phenol on $\text{TiO}_2/\text{SiO}_2$ is investigated in order to explain its role in the photocatalytic process. Finally, experiments were performed to prove the possibility of total phenol mineralization, *i.e.* the photooxidation to CO_2 and H_2O .

Results and Discussion

Photocatalytic reactions, both continuous and non-continuous, were conducted in a fluidized bed reactor using an air lift controlled by a draft tube described previously [33]. The diagram of the reactor is shown in Fig. 1. The draft tube provides bulk circulation of gas, liquid, and solid inside the reactor. This assures, in turn, high gas holdup and high contact efficiency between the gas phase and the liquid phase as well as between the liquid phase and the solid phase [34]. Any powder photocatalyst can be utilized in the reactor when it operates in the non-continuous mode, *e.g.* TiO_2 Degussa P-25. However, in the continuous operation the separation

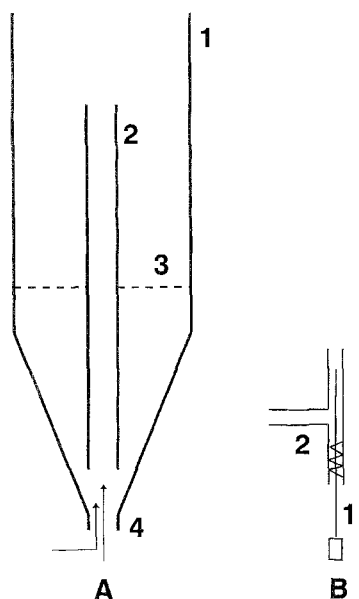


Fig. 1. A: photoreactor; 1: external tube, 2: internal (draft) tube, 3: draft tube bearers, 4: air and water injector; B: air and water injector; 1: air injector, 2: water supplying pipe

of the solid from the solution requires special photocatalyst grains of larger size. Therefore, fine titania powder (Degussa P-25) has been strongly attached to appropriate silica gel grains (Aldrich, 30–60 mesh).

The light efficiency in small photochemical cells like that employed in the present investigation (110 ml volume) is rather poor. It can be improved by scaling up the photoreactor and using immersed lamps. In addition to the problem of the best light utilization which is not considered in the present paper, two factors influence the efficiency of a photoreactor: the amount of catalyst and the air flow rate responsible for liquid and solid circulation within the photoreactor. The flow rate of the liquid is very low and should not influence appreciably the hydrodynamic conditions. It was checked in separate experiments that both the amount of catalyst and the air flow rate are characterized by threshold values: the yields of photocatalytic reactions decrease below the thresholds, and they become constant above the thresholds. Thus, 0.7 g $\text{TiO}_2/\text{SiO}_2$ and an air flow rate of 7.11 h^{-1} were chosen as the optimum values for further experiments.

Figure 2 shows yield of phenol vs. time at a moderate phenol flow rate (96.2 ml.h^{-1}). In this case, steady state conditions were obtained after about 2 h. Shorter times were observed at higher flow rates when the yields of the photoreaction were lower. The short vertical lines in Fig. 2 indicate the scattering of the results of 5 subsequent experiments. It can be seen that under steady-state conditions, *i.e.* in the reaction period from 120 to 360 min, the results vary within less than 10%. Considering several factors that influence the rate of phenol photodegradation (like liquid and air flow rates, precision of GC measurements, *etc.*), the accuracy of the reaction yield evaluation seems to be sufficiently good.

Figure 3 shows phenol photodecomposition rates (in % of initial phenol content) vs. feed flow rates. All other factors were kept constant. Each point in Fig. 3 expresses an average yield of phenol decomposition in the reaction period of 120–360 min, *i.e.* under steady-state conditions. Certainly, low flow rates favour

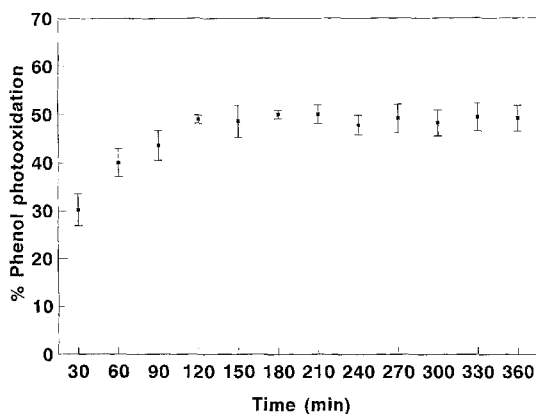


Fig. 2. Phenol photodecomposition (in %, continuous mode) vs. time; the lines express the discrepancy of results of five subsequent experiments; conditions: phenol concentration, $1 \cdot 10^{-4}$ mol/l; phenol flow rate, 96.2 ml/h; amount of $\text{TiO}_2/\text{SiO}_2$, 0.7 g; air flow rate, 7.1 l/h; temperature, $33 \pm 1^\circ\text{C}$

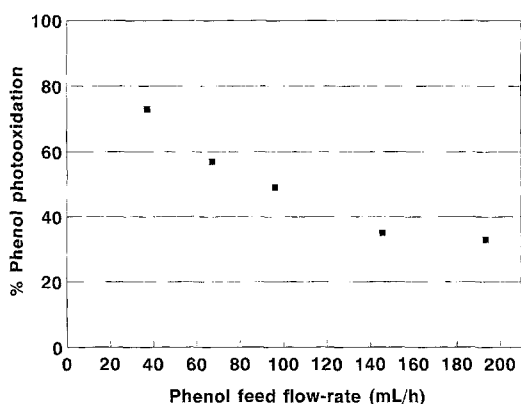


Fig. 3. Steady-state phenol photodecomposition (in %) vs phenol feed flow rate continuous mode; conditions: phenol concentration, $1 \cdot 10^{-4}$ mol/l; air flow rate, 7.1 l/h; amount of $\text{TiO}_2/\text{SiO}_2$, 0.7 g; temperature, $33 \pm 1^\circ\text{C}$

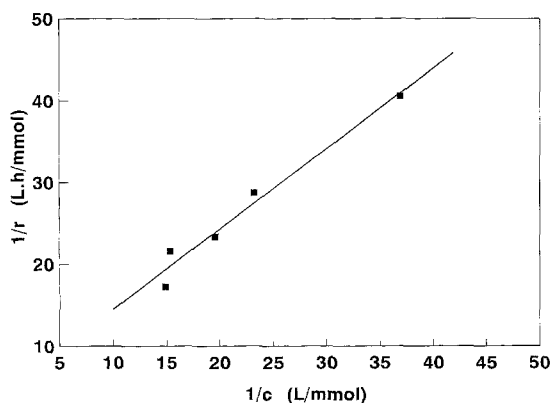


Fig. 4. Rate of steady-state phenol photo-decomposition vs phenol feed flow rate, continuous mode; for reaction conditions, see Fig. 3

higher degrees of phenol disappearance since the residue times are higher. For example, at a flow rate of $37.1 \text{ ml} \cdot \text{h}^{-1}$ only 27% of the initial amount of phenol remained in the outgoing solution (yield: 73%). Under these conditions, the solution in the reactor was renewed after 3 h. At a high phenol flow rate, when the reactor solution was renewed nearly twice in 1 h, 33% phenol decomposition was observed. However, the reaction rates at higher flow rates were bigger due to the high phenol equilibrium concentration under steady-state conditions (Fig. 4).

It is well known that phenol photodecomposition in the presence of titania obeys 1st order kinetics [27]. Hence, the rate constants can be calculated from the *Langmuir-Hinshelwood* equation

$$\frac{1}{r} = \frac{1}{k} + \frac{1}{k \cdot K_{\text{ads}} \cdot c}$$

where r is the reaction rate, k is the reaction rate constant, K_{ads} is the equilibrium adsorption constant, and c is the substrate concentration. If the plot $1/r$ vs. $1/c$ is linear, both k and K_{ads} can easily be calculated: $k = 0.214 \text{ mmol} \cdot \text{dm}^{-3} \cdot \text{h}^{-1}$ and $K_{\text{ads}} = 4.77 \text{ dm}^3 \cdot \text{mmol}^{-1}$ based on the data of Fig. 4. The calculation procedure is simplified in the case of a continuous process when steady-state conditions are attained. Here, c is the phenol concentration in the outgoing water measured by any analytical technique. On the contrary, in non-continuous methods (batch reactors) initial reaction rates have to be evaluated from rate vs. time plots. Therefore, the continuous photocatalytic process can be recommended for simple calculations of kinetic constants.

Adsorption studies have been performed in order to establish if K_{ads} , calculated from kinetic data of the photocatalytic process, can be regarded as the real adsorption equilibrium constant. Note that the same rate expression equation could be applied independently on the mechanism of the photocatalytic phenol decomposition on titania as shown by *Turchi and Ollis* [27]. First, it was necessary to establish conditions for an adsorption equilibrium. The results given in Fig. 5 show that – although initially the adsorption is fast – the equilibrium is accomplished after about 90 min. Therefore, in all further experiments, 120 min adsorption time was applied as a standard to ensure real equilibrium conditions. Amounts of phenol adsorbed vs. equilibrium concentration, both for $\text{TiO}_2/\text{SiO}_2$ and, for comparison, for silica gel alone, are shown in Fig. 6. The amount of phenol adsorbed on 1 g $\text{TiO}_2/\text{SiO}_2$ is low even at the highest equilibrium concentration: $0.043 \text{ mg} \cdot \text{g}^{-1}$ ($0.5 \text{ } \mu\text{mol} \cdot \text{g}^{-1}$) at $c_{\text{eq}} = 0.57 \cdot 10^{-4} \text{ mol} \cdot \text{l}^{-1}$. However, the value looks reasonable compared to literature data: $3.5 \text{ } \mu\text{mol} \cdot \text{g}^{-1}$ were reported by *Cunningham and Sedlak* [28], and about $10 \text{ } \mu\text{mol} \cdot \text{g}^{-1}$ were observed by *Trillas et al.* [11]. Both values refer to adsorption of phenol on TiO_2 P25 Degussa. The much lower

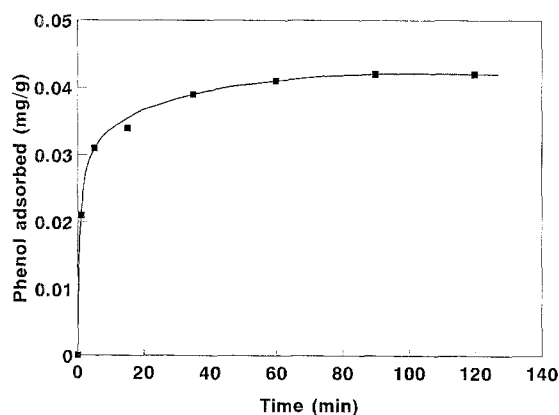


Fig. 5. Phenol adsorption on $\text{TiO}_2/\text{SiO}_2$ vs. time; Adsorption condition: phenol concentration, $1 \cdot 10^{-4} \text{ mol/l}$; amount of solution, 10 ml; temperature, $22 \pm 1^\circ\text{C}$

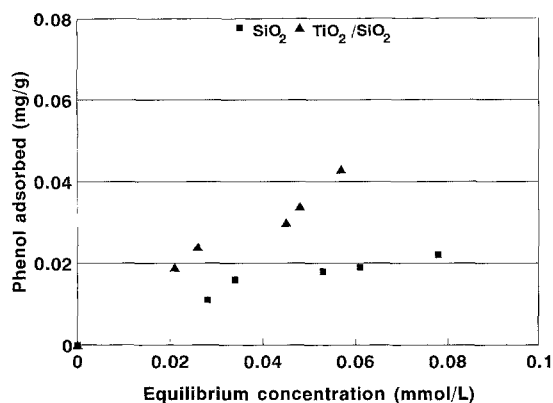


Fig. 6. Phenol adsorption on TiO₂/SiO₂ and SiO₂ vs. phenol equilibrium concentration; adsorption conditions: amount of SiO₂ and TiO₂/SiO₂, varying between 1 and 2 g; phenol concentration, varying between 0.5·10⁻⁴ and 1·10⁻⁴ mol/l; amount of solution, 10 ml; adsorption time, 2 h

values reported here are due to the fact that 1 g TiO₂/SiO₂ contains only 0.05 g of titania. Note that the adsorption on the silica gel alone is rather poor (Fig. 6).

For diluted solutions, K_{ads} can be calculated from the ordinary *Langmuir* adsorption isotherm (see *e.g.* Ref. [35]). Thus, based on the results shown in Fig. 3, the calculated K_{ads} for phenol adsorption on TiO₂/SiO₂ amounts to 12.8 dm³ · mmol⁻¹. Compared to $K_{\text{ads}} = 4.77$ dm³ · mmol⁻¹, calculated from the 1st order kinetic expression for the photocatalytic reaction, the above value is about 2.7 times higher. The difference between these two values can be rationalized in several ways. First, the adsorption data refer to the whole surface of TiO₂/SiO₂, whereas these taken from the photoreaction data to titania alone. Second, the mechanism of the photoprocess is complicated and involves, besides the reaction of holes or OH radicals with phenol molecules, also various reactions of these species with intermediates which adsorb competitively on TiO₂ (see below). Finally, the photooxidation of phenol can proceed at the same time on the semiconductor surface and in the bulk solution *via* free OH radicals. Therefore, although the above results seem to confirm the influence of phenol adsorption on the overall rate of the photoreaction, it is impossible to evaluate the extent of the dependence.

Total phenol photomineralization was studied in the non-continuous mode. In these experiments, a 4·10⁻⁴ m phenol solution was used for two reasons: (i) the rate of phenol decomposition was slower and its time dependence easier to determine, and (ii) HPLC and TOC analysis were more accurate at the higher concentration. It should be added here that, in addition to HPLC, GC analysis of phenol was also performed. Phenol photodetoxification rates measured both by HPLC (and GC) and TOC are presented in Fig. 7. The difference between the HPLC (or GC) and TOC results expresses the amount of phenol converted photocatalytically into organic intermediates. It follows from Fig. 7 that as much as 20% of the initial phenol exist as organic intermediates. The intermediates undergo finally total mineralization as could be observed in some long time experiments. Attempts have been undertaken to determine the intermediates by GC (fused silica capillary column, programmed temperature 40–300°C), HPLC (conditions: see Experimental), and UV/Vis spectrophotometry (180–1000 nm). Unfortunately, the efforts were not successful. None of the intermediates accepted in the literature like hydroquinone, benzoquinone, or catechol (see *e.g.* Ref. [36]) nor other compounds could be detected. However, taking into account the rather great difference between HPLC

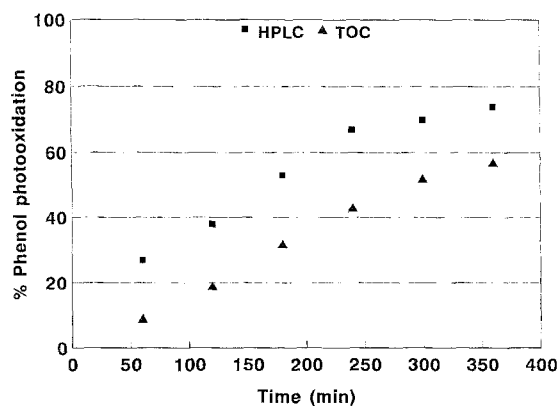


Fig. 7. Phenol Photodecomposition vs. time, non-continuous mode; phenol disappearance was measured using both HPLC (and, for comparison, GC) and TOC; conditions: phenol concentration, $4 \cdot 10^{-4}$ mol/l; initial pH, 6; amount of $\text{TiO}_2/\text{SiO}_2$, 0.7 g; reaction temperature, $33 \pm 1^\circ\text{C}$; air flow rate, 7.1 l/h

(and GC) and TOC results and literature data on phenol photooxidation, we would like to mention here our hypothesis concerning possible reaction intermediates.

In the literature, photooxidation of phenol has been regarded as a process involving cyclohexadienyl [31] or phenoxy [31, 32, 37, 38] radicals, with a stress on the latter one in more recent literature [31, 32]. On the other hand, the formation of dimeric or polymeric compounds during oxidation is well known in the chemistry of phenolic compounds (see *e.g.* Ref.[39] and Refs. cited therein). For example, the phenoxy radicals ($\text{C}_6\text{H}_5\text{O}$) can easily react to dihydroxyphenyls, diphenoquinones, ethers, or polyethers. Also, the products of phenol oxidation can form polymers [39]. The dimeric and polymeric compounds are hardly water soluble. Some of them can be coloured. In the experiments, the colourless solution turned reddish-brown as a consequence of illumination. At the same time, the surface of the white $\text{TiO}_2/\text{SiO}_2$ changed to reddish-brown obviously due to the adsorption of the polymers. The failure to detect such polymers is not surprising. They are not volatile enough to be detected by GC and cannot be detected by HPLC and UV/Vis spectrophotometry due to their poor solubility. Therefore, we postulate here that photooxidation of phenol leads to the formation of intermediates, mainly to di- and/or polymeric compounds. Oxidation of the intermediates by illuminated titania to yield CO_2 and H_2O competes with oxidation of the phenol substrate. Finally they undergo total mineralization as could be observed in some experiments. The hypothesis concerning polymeric intermediates, although it seems to be likely, needs experimental proof. At present, studies to elucidate the role of intermediates like hydroquinone, benzoquinone, catechol and to proof (or reject) the above hypothesis are in progress.

Conclusions

The studies of photocatalytic phenol degradation were performed in the original reactor proposed by the authors using an air lift controlled by a draft tube. The reactor can operate both in continuous and non-continuous mode. In this investigation, the kinetics of the photocatalytic reaction were measured under flow conditions; it is, to our knowledge, the first report dealing with the kinetics of continuous water photodetoxification.

Adsorption of phenol on TiO_2 is fast and therefore takes place also during photocatalytic reaction and influences the reaction rate. However, basing on our data, it is impossible to state precisely the influence of the adsorption on the overall rate of phenol photodecomposition. The photocatalytic process leads primarily to intermediates that are finally fully mineralized. It is postulated that the intermediates consist mainly of polymeric compounds, difficult to determine using conventional methods like GC, HPLC, and UV/Vis spectroscopy.

Experimental

The photocatalyst

2.5 g TiO_2 (Degussa P25) were added to 80 ml H_2O and sonicated for 20 min. Next, the titania slurry was mixed with 47.5 g silica gel (Aldrich, 30–60 mesh) in a round bottom flask, and the water was evaporated in a rotary vacuum evaporator at 90°C . The dry powder was calcinated 6 h in air at 400°C . The XRD spectrum of the thus prepared $\text{TiO}_2/\text{SiO}_2$ showed only lines characteristic for TiO_2 Degussa P25, *i.e.* a mixture of anatase and rutile with a ratio of 80:20, in addition to a broad band of amorphous silica. A more detailed analysis has been given in an earlier paper [40].

Photocatalytic studies

The experiments were performed in continuous and non-continuous modes in a photoreactor similar to that described before [33]. For the design of the gas-solid-liquid photoreactor we relied on known geometries used in chemical industry for mixing systems and reactors using an air lift controlled by a draft tube; for details, see *e.g.* Refs. [41–44]. A diagram of the photoreactor is given in Fig. 1A; the air and liquid injector is shown in Fig. 1B. Both air and liquid were supplied at the bottom of the reactor. The water outlet tube (not shown) was located inside the reactor near the wall, with the bottom close to the conical section and the exit located 15 mm below the top of the reactor. The Dimensions of the reactor have been given before [33]. The total volume of the photoreactor amounted to 110 ml.

Both air and phenol solution were supplied using silicon rubber tubes. The air flow rate was controlled by a rotameter. The solution of phenol was fed into the reactor using a peristaltic pump. The photoreactor was placed inside a Pyrex-made water bath whose temperature was controlled and maintained at $33 \pm 1^\circ\text{C}$. The reactor was illuminated from a side wall with light from a high pressure Hg lamp (125 W, Philips). The Pyrex walls of both the photoreactor and the water bath determined a lower limit of the wavelength of entering light (about 300 nm cutoff filter). The incident light flux was $1.15 \mu\text{mol quanta/s}$ as measured by uranyl-oxalic actinometry [45].

During the experiment, the photoreactor was filled with 110 ml of phenol solution, mostly 1.10^{-4} M , using a peristaltic pump (phenol, 99% purity, was supplied by Aldrich). An air flow of usually $119 \text{ ml}\cdot\text{min}^{-1}$ was applied, and illumination was started. After the temperature of the water bath had been adjusted at 33°C , an appropriate amount of $\text{TiO}_2/\text{SiO}_2$ (usually 0.7 g) was added to the solution. The air and liquid flow rates and the water bath temperature were kept constant, and the photoreaction (continuous mode) was conducted for 6 h. All exceptions from the above conditions are marked in the Results and Discussion section. The phenol concentration was determined in the solution leaving the reactor by GC (Hewlett Packard Model 5830, 30 m fused silica capillary column, FID detector) after filtration over Millipore Millex GV₃ filter units. In some cases the solution was analyzed additionally by TOC using a Dohrmann DC-190 high temperature TOC analyzer and HPLC (waters, model 501 using OD S2 5 μm column, 1:1 water-acetonitrile, UV detector working at 270 nm).

In the case of non-continuous phenol photodecomposition, 110 ml of an appropriate phenol solution was poured into the reactor, and an air stream was applied. The further procedure was similar to that in the case of the continuous method. For phenol analysis, 0.5 ml of the reaction solution were withdrawn every 30 or 60 min with a syringe; after filtration over the Millipore filter, the phenol concentration was determined as described previously.

Details of the experimental procedures (phenol concentration, air and liquid flow rates, amount of the catalyst, mode of the reaction (continuous or non-continuous), mode of determination of phenol destruction rates) are given together with adequate results (see captions to Figs.). In all experiments, Millipore 18 Mohm water was used. All reactants were of *p.a.* purity.

Adsorption studies

10 ml of phenol solution were poured into small glass vials, and an appropriate amount of TiO₂/SiO₂ of silica gel was added. The silica gel was calcinated before 6 h in air at 400°C. The vials were closed and kept in the dark at 22±1°C. The contents of the vials were shaken every 5 min. The phenol solution was withdrawn from the vials with a syringe after 2 h of adsorption (except time-dependence experiments), and the catalyst grains were separated on a Millipore filter. The phenol concentration was determined by GC (see above).

Acknowledgements

The authors are grateful to the *Comision Interministerial de Ciencia Y Tecnologia (CICYT)* (project AMB92-1021-C02-01) and to *Plataforma Solar de Almeria - IER-CIEMAT* (project 11/94) for funds to perform this work. Financial support to A.S. from *Direccio General d'Universitats del Departament d'Ensenyament de la Generalitat de Catalunya* and from *Subdireccion General de Promocion de la Investigacion* of Spanish Ministry of Education and Science during his stay at the University of Barcelona is gratefully acknowledged.

References

- [1] Matthews RW (1992) *Pure Appl Chem* **64**: 1285
- [2] Fox MA, Dulay MT (1993) *Chem Rev* **93**: 341
- [3] Wold A (1993) *Chem Mater* **5**: 280
- [4] Pelizzetti E, Minero C (1993) *Electrochim Acta* **38**: 47
- [5] Legrini O, Oliveros E, Braun AM (1993) *Chem Rev* **93**: 671
- [6] Oppenlaender T, Baun G, Egle W (1994) *EPA Newsl* **52**: 33
- [7] Sobczynska A, Sobczynski A (1994) *Pol J Appl Chem* **38**: 25
- [8] Jacob L, Oliveros E, Legrini O, Braun AM (1993) TiO₂ Photocatalytic Treatment of Water. In: Ollis DF, Al-Ekabi H (eds) *Photocatalytic Purification and Treatment of Water*. Elsevier, Amsterdam, p 511
- [9] Gimenez J, Aguado MA, Cervera S, Borell L, Curco D, Queral MA (1994) Photoreactor Design for Photocatalytic Detoxification. In: Klett DE, Hogan RE, Tanaka T (eds) *Solar Engineering*. The American Society of Mechanical Engineers, New York, p 139
- [10] Blanco J, Malato S (1994) Solar Photocatalytic Mineralization of Rest-Hazardous Waste Water at Preindustrial Level. In: Klett DE, Hogan RE, Tanaka T (eds) *Solar Engineering*. The American Society of Mechanical Engineers, New York, p 103
- [11] Trillas M, Pujol M, Domenech X (1992) *J Chem Technol Biotechnol* **55**: 85
- [12] Abdullah M, Low GKC, Matthew RW (1990) *J Phys Chem* **94**: 6820
- [13] Takeda N, Torimoto T, Kuwabota S, Yonegama H (1995) *J Phys Chem* **99**: 9989
- [14] Diller R, Brandt M, Fornefelt I, Siebers U, Bahnemann D (1995) *Chemosphere* **30**: 2333

- [15] Hidaka H, Zhao J, Pelizzetti E, Serpone N (1992) *J Phys Chem* **96**: 2226
- [16] Muszkat L, Bir L, Feigelson L (1995) *J Photochem Photobiol A* **87**: 85
- [17] Mao Y, Schoeneich C, Asmus KD (1991) *J Phys Chem* **95**: 10080
- [18] Sitkiewitz S, Heller A (1996) *New J Chem* **20**: 233
- [19] Monaci A, Ginstra A (1996) *J Photochem Photobiol A* **93**: 199
- [20] Tahiri H, Serpone N, Mao RL (1996) *J Photochem Photobiol A* **93**: 199
- [21] Terzian R, Serpone N, Hidaka H (1995) *Catal Lett* **32**: 227
- [22] Ku Y, Hsieh CB (1992) *Ind Eng Chem Res* **31**: 1823
- [23] Zang L, Liu CY, Ren XM (1995) *J Chem Soc Faraday Trans* **91**: 917
- [24] Minero C, Pelizzetti E, Pichat P, Sega M, Vincenti M (1995) *Environ Sci Technol* **29**: 2226
- [25] Prousek J, Slarikova M (1996) *Chem Listy* **90**: 829
- [26] Mills A, Morris S, Davies R (1993) *J Photochem Photobiol A* **70**: 183
- [27] Turchi CS, Ollis DF (1990) *J Catal* **122**: 202
- [28] Cunningham J, Sedlak P (1993) Initial Rates of TiO₂ Photocatalysed Degradation of Water Pollutants: Influences of Adsorption, pH and Foton Flux. In: Ollis DF, Al-Ekabi H (eds) *Photocatalytic Purification and Treatment of Water and Air*. Elsevier, Amsterdam, p 67
- [29] Matthew RW (1988) *J Catal* **113**: 549
- [30] Lawless D, Serpone N, Meisel D (1991) *J Phys Chem* **95**: 5166
- [31] Goldstein S, Czapski G, Rabani J (1994) *J Phys Chem* **98**: 6586
- [32] Stafford U, Gray KA, Kamat PV (1994) *J Phys Chem* **98**: 6343
- [33] Sobczyński A, Gimenez J, Cervera-March S (1996) *Pol J Appl Chem* **40**: 103
- [34] Fan LS, Hwang SJ, Matsuura A (1984) *Chem Eng Sci* **39**: 1677
- [35] *Perrys Chemical Engineer's Handbook*, 6th edn (1984) Mc Graw-Hill, chapter 16, p 12
- [36] Matthew RW (1984) *J Chem Soc Faraday Trans* **80**: 457
- [37] Fox MA (1993) The Role of Hydroxyl Radicals in the Photocatalysed Detoxification of Organic Pollutants: Pulse Radiolysis and Time-Resolved Diffuse Reflectance Measurements. In: Ollis DF, Al-Ekabi H (eds) *Photocatalytic Purification and Treatment of Water and Air*. Elsevier, Amsterdam, p 163
- [38] Drapper RB, Fox MA (1990) *Langmuir* **6**: 1990
- [39] *Rodd's Chemistry of Carbon Compounds*, 2nd edn (1971) Elsevier, Amsterdam, vol III, part A, p 298
- [40] Escudero JC, Simarro R, Cervera-March S, Gimenez J (1989) *Chem Eng Sci* **44**: 583
- [41] Sterbacek Z, Tausk P (1965) *Mixing in the Chemical Industry*. Pergamon Press, Oxford London
- [42] Elvers B, Hawkins S, Schulz G (eds) VCH, (1992) *Ullman's Encyclopedia of Industrial Chemistry* 5th edn. Weinheim, vol B4
- [43] Eccles RM, De Vaux GR (1981) *Chem Eng Prog* **77**(5): 80
- [44] Steiner R (1987) *Chem Eng Process* **21**: 1
- [45] Murov SL (ed) (1973) *Handbook of Photochemistry*. Dekker, New York

Received February 10, 1997. Accepted (revised) June 13, 1997